ORIGINAL ARTICLE

# Bending performance of concrete with coarse recycled aggregate and raw-crushed wind-turbine blade at an early age

**Vanesa Ortega-López[1,2] · Flora Faleschini[2] · Juan M. Manso[1] · Víctor Revilla-Cuesta[1,2]**

Received: 15 January 2025 / Revised: 11 April 2025 / Accepted: 2 May 2025


## Abstract

The bonded mortar in the Coarse Recycled Aggregate (CRA) reduces both the adhesion in the interfacial transition zones and the stiffness of concrete, which worsens concrete bending behavior. These aspects are more remarkable at early ages due to the lower strength and stiffness developed by the concrete matrix. The stitching effect of the 66.8% by weight of Glass Fiber-Reinforced Polymer (GFRP) fibers contained in Raw-Crushed Wind-Turbine Blade (RCWTB) can counteract these phenomena. This research analyzes the bending behavior of concrete made with up to 100% CRA in combination with 6% RCWTB as aggregate replacement. Early ages (1, 3, and 7 days) and both moist and ambient curing are considered to cover all possible put-into-service situations of concrete elements. Compared to concrete with the same composition but without RCWTB, this waste increased the pre-failure compliance by up to 26.9%, the failure deflection by up to 12.8%, and the failure stress by up to 37.5% when combined with as much as 50% CRA. An earlier concrete age and ambient curing made such effects more notable due to the weaker cementitious matrix. Furthermore, RCWTB provided post-failure load-bearing capacity to concrete, the incorporation of 6% RCWTB to concrete with 50% CRA increasing the absorbed energy under bending loading by 135%. RCWTB also allowed the energy absorbed by concrete to be almost unaffected when adding any CRA amount. All these effects were statistically significant and demonstrate that RCWTB improves the bending deformability of concrete produced with CRA, mainly because of the deflection improvement it caused.

**Keywords** Raw-crushed wind-turbine blade · Coarse recycled aggregate · Concrete · Load–deflection test · Deformability · Energy absorption

## Abbreviations

| | |
|---|---|
| ANOVA | Analysis of variance |
| CNA | Coarse natural aggregate |
| CRA | Coarse recycled aggregate |
| GFRP | Glass fiber-reinforced polymer |
| ITZs | Interfacial transition zones |
| RCWTB | Raw-crushed wind-turbine blade |


https://doi.org/10.1007/s43452-025-01215-5

Published online: 16 May 2025

## 1 Introduction

Concrete is a building material mainly characterized by a high compressive strength [1], thereby being used for the construction of a wide variety of elements primarily subjected to compressive stresses [2]. However, concrete is also used for the design of numerous elements that work under bending conditions, such as beams [3] or pavements [4], in which tensile stresses appear. Since concrete does not withstand high levels of tensile stresses, steel reinforcement bars are usually placed in the tensile zone of the element to improve such behavior [5]. They also help to limit concrete deflections and reduce its brittleness by increasing the energy absorbed during loading [6]. In this way, the use of any concrete element working in bending is more comfortable and safer [7], being the element even able to bear certain load levels after a sudden failure [8]. However, the better the behavior of plain concrete without reinforcement in bending terms, the lower the amount of reinforcement required, which leads to economic savings and greater sustainability of the concrete structure [9].

There are numerous wastes that can be used as raw materials for concrete manufacturing [10], which impact the performance of concrete in many dimensions [11], bending behavior being among them [12]. One of the most common and widely researched wastes is the aggregate from out-of-use crushed concrete [13]. This material can be used as both coarse and fine aggregate [14], the use of the latter being more problematic for the bending performance of concrete due to its high content of fine mortar particles [15]. However, Coarse Recycled Aggregate (CRA) also affects such behavior of concrete. On one hand, the bonded mortar makes the CRA particles more flexible than those of Coarse Natural Aggregate (CNA), which reduces concrete stiffness when loaded [16]. On the other hand, the bonded mortar also decreases the bond between the cementitious matrix and the aggregates in the Interfacial Transition Zones (ITZs) [17], which causes the concrete to fail at lower load levels and, sometimes, in a more brittle way [18]. The higher water/cement ratio of concrete when CRA is added to compensate for the loss of workability because of the irregular shape and the high water-absorption levels of CRA [19] weakens the cementitious matrix due to the increased porosity that water evaporation causes [20], which also favors these phenomena [21].

The addition of fibers to concrete is a relatively recent technology that improves the bending behavior of concrete. The fibers act as a three-dimensional reinforcement of the cementitious matrix that provides a stitching effect [22]. Thus, they increase pre-failure stiffness of concrete when their elastic modulus is high enough [23] and, in some cases, the failure stress [24]. In addition, they contribute to a less brittle concrete failure, as the fibers are capable of supporting load in collaboration with the compressed zone of the concrete element once the failure has occurred [4]. This generic behavior is modified by the particularities of each fiber type. For example, steel fibers show greater advantages than polymeric fibers, usually polypropylene fibers, since they have a higher elastic stiffness that reduces their strain at the same stress level [25]. The use of recycled or natural fibers is another possibility [26], which exhibit similar advantages to conventional fibers, and at the same time reduce the environmental impact of fiber production [27]. Different fiber types, such as basalt [28], glass [29] and natural [30] fibers, are effective in improving the behavior of concrete with CRA.

Glass Fiber-Reinforced Polymer (GFRP) is a composite with a great number of applications because it offers a balance between strength and weight [31]. However, its composition based on fiberglass embedded in a polymeric matrix, generally based on an epoxy resin, hinders its recycling at the end of its useful life [32]. One possibility is to separate the glass fibers from the polymeric matrix by means of chemical or thermal treatments [33], although these procedures significantly deteriorate the mechanical properties of the glass fibers, which limits their subsequent use [34]. In addition, these processes emit high amounts of greenhouse gases into the atmosphere and are energy-intensive [35]. As a result, mechanical recycling of GFRP is currently an interesting alternative [31]. In this way, GFRP is crushed in knife mills, resulting in GFRP fibers, composed of both fiberglass and polymer resin, which can be added to concrete [36]. GFRP fibers may increase elastic stiffness when added in high amounts, and improve the strength of concrete and its load-bearing capacity under bending [37], performance also found when combined with CRA in concrete [38].

The problem of GFRP recycling can be even more pronounced if it is combined with other materials. Wind-turbine blades are a good example [39], in which GFRP is sandwiched and interlayered with balsa wood and different types of polymers [40]. These components reduce the weight of the blade, glue elements between them, and even internally stiffen the hollow section of the blade [41]. GFRP from wind-turbine blades can be recycled as indicated in the previous paragraph, but a prior separation of the GFRP from the other components is necessary, which hinders the process [39]. The simultaneous crushing of all the elements of wind-turbine blades results in a material with a high proportion of GFRP fibers [42], and also with particles of polymers and balsa wood [43] that do not prevent the GFRP fibers to successfully contribute to an improved bending performance of concrete [44]. This material has been named Raw-Crushed Wind-Turbine Blade (RCWTB) in previous research [43], whose efficacy in concrete containing CRA under bending conditions has not yet been scientifically evaluated.

This study analyzes the bending behavior of concrete produced with variable CRA contents between 0 and 100% by volume of coarse aggregate and 6% RCWTB, and compares it with concrete mixes of identical composition, but without RCWTB. Deformational, strength and energy-absorption features are considered. In addition, this analysis is conducted at an early age of concrete (1, 3, and 7 days) and for both moist and ambient curing, with the aim of simulating as accurately as possible the conditions under which the concrete elements are put into service. None of these aspects have been previously analyzed in scientific research. The final goal is to elucidate whether RCWTB can improve the bending performance of concrete with CRA. A suitable performance would allow progress in the simultaneous revaluation of two wastes from the dismantling of wind farms, the RCWTB from the wind-turbine blades and the CRA from the demolition of the wind-turbine footings, through their use as raw materials in concrete.

## 2 Materials and methods

### 2.1 Raw materials

The conventional ingredients of concrete in this study were CEM II/A-L 42.5 R Portland cement following EN 197–1 [45]; ordinary tap water; two modified-polycarboxylate plasticizers, one of them water-based, which showed good performance in previous research on concrete containing RCWTB [44]; siliceous aggregate of sizes 12–22 mm, 4–12 mm, and 0–4 mm, with densities between 2.60 kg/dm$^3$ and 2.63 kg/dm$^3$ and 24-h water-absorption levels between 0.13% and 0.55% as *per* EN 1097–6 [45]; and limestone sand of size 0–2 mm with a density and 24-h water absorption of 2.66 kg/dm$^3$ and 0.10%, respectively. The gradation of all these aggregates is depicted in Fig. 1.

Recycled aggregate was obtained by jaw crushing a parent concrete with a compressive strength higher than 45 MPa. A subsequent sieving allowed obtaining the CRA 4–22 mm used in this research (Fig. 2a) to partially or totally replace the CNA. The density of CRA was 2.44 kg/dm$^3$, and its 24-h water absorption was

**Fig. 1** Gradation of aggregates according to EN 933–1 [45]

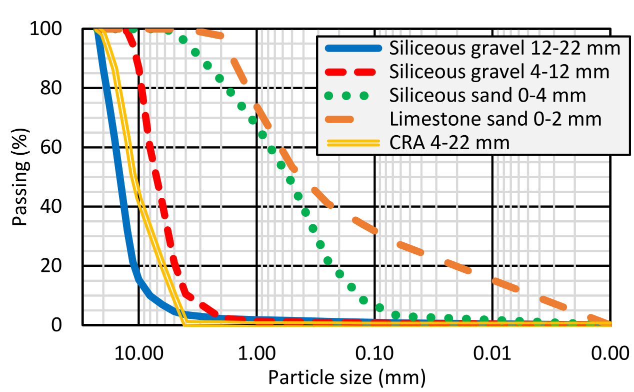

 https://doi.org/10.1007/s43452-025-01215-5


**Fig. 2** Wastes used in concrete: **a** CRA 4–22 mm; **b** RCWTB

6.12%. As expected, the CRA was less dense and more water-consuming than the CNA [46]. The gradation of the CRA was also adequate for concrete manufacturing (Fig. 1).

Panels from the walls of a wind-turbine blade were knife crushed and screened through a 10-mm-aperture sieve to yield RCWTB (Fig. 2b). This material presented a complex composition, which is shown in Fig. 3. It was mainly characterized by a content of 66.8% by weight of GFRP fibers, whose physical–mechanical properties are detailed in Table 1. The density of RCWTB according to EN 1097-6 [45] was 1.63 kg/dm$^3$. A more comprehensive characterization of this residue can be found in a previous publication [43].

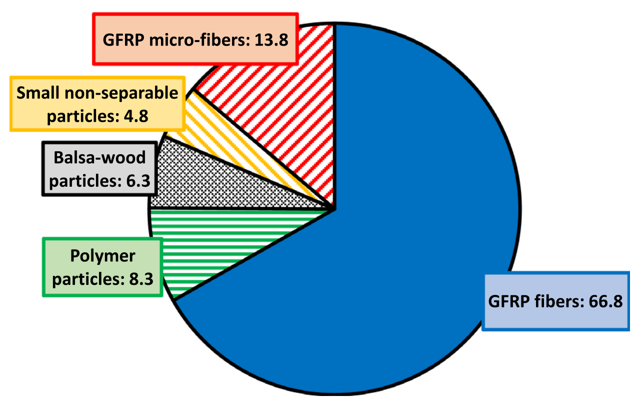


**Fig. 3** RCWTB composition (% wt.) by adapting EN 933–11 [45]

**Table 1** Physical–mechanical properties of GFRP fibers present in RCWTB

| Property | Value | Standard [45, 47] |
|---|---|---|
| Real density (kg/dm$^3$) | 2.04 | EN 1097–6 |
| Tensile strength (MPa) | 270 | EN ISO 6892–1 |
| Average length (mm) | 13.1 | ASTM D5103 |
| Average diameter (mm) | 0.73 | ASTM D2130 |
| Aspect ratio (dimensionless) | 18 | ASTM D5103, ASTM D2130 |

**Table 2** Composition of the concrete mixes (kg/m$^3$)

| Mix | Cement | Water | Plasticizers[1] | Limestone sand | Siliceous aggregate[2] | CRA | RCWTB |
|---|---|---|---|---|---|---|---|
| *0CRA/0RCWTB* | 320 | 130 | 3.20 | 280 | 780 # 555 # 385 | 0 | 0 |
| *50CRA/0RCWTB* | 320 | 140 | 3.20 | 280 | 390 # 277 # 385 | 623 | 0 |
| *100CRA/0RCWTB* | 320 | 150 | 3.20 | 280 | 0 # 0 # 385 | 1246 | 0 |
| *0CRA/6RCWTB* | 320 | 130 | 3.20 | 263 | 733 # 522 # 362 | 0 | 71 |
| *50CRA/6RCWTB* | 320 | 140 | 3.20 | 263 | 367 # 261 # 362 | 586 | 71 |
| *100CRA/6RCWTB* | 320 | 150 | 3.20 | 263 | 0 # 0 # 362 | 1171 | 71 |

[1]Plasticizers were in a 2:1 ratio

[2]Amounts of siliceous aggregate in the fractions 12/22 mm # 4/12 mm # 0/4 mm

**Fig. 4** Overall gradation of concrete mixes

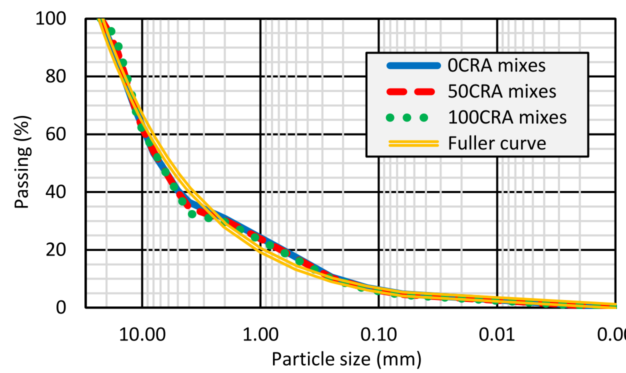


## 2.2 Concrete composition

Six concrete mixes were prepared to evaluate the effect of CRA and RCWTB on the bending concrete performance:

- Three concrete mixes incorporated CRA contents of 0%, 50%, and 100% with respect to the total volume of coarse aggregate and did not contain RCWTB. Their aim was to evaluate the effect of different CRA amounts on the bending performance of concrete, as in other research [3].
- The other three concrete mixes incorporated a RCWTB content of 6% of the total volume of aggregates, amount that was defined on the basis of previous results that showed the improvement of the flexural strength of concrete with such waste content [44]. Each mix had a different CRA content (0%, 50%, and 100%) to compare them with the mixes without RCWTB, thus evaluating the interactions between both wastes [38].

  The composition of all the mixes is shown in Table 2, following their labelling the format "*XCRA/YRCWTB*", where *X* and *Y* represent the percentage content of CRA and RCWTB, respectively.

The design of the mixes was based on a cement content of 320 kg/m$^3$, a water/cement ratio of 0.40, and a plasticizer content of 1% of the cement mass. The overall aggregate gradation was defined through the adjustment to the Fuller curve (Fig. 4), which allows a proper balance between aggregate packing and aggregate-fines content, thus simultaneously yielding proper workability and strength levels in the concrete produced with wastes [43]. All these aspects were intended to develop a concrete widely suitable for structural use [5], *i.e.*, with a slump class S3 according to EN 206 [45] and a compressive strength higher than 45 MPa. These design features were modified as little as possible when adding CRA and RCWTB so as not to introduce additional factors that would affect the results obtained. Therefore, the cement and plasticizer contents were not modified upon addition of the by-products. Besides, the gradation of the CRA was adequate so that its incorporation did not alter the overall gradation of concrete, as detailed in Fig. 4. Finally, the water/cement ratio was minimally increased following the addition of CRA so that its higher water absorption was compensated for and the effective water/cement ratio of concrete remained constant [19].

## 2.3 Experimental program

The bending behavior of the mixes was evaluated by performing load–deflection tests on 75 × 75 × 275 mm specimens, the test setup being shown in Fig. 5. In this test, the specimen was placed simply supported and centered on two rollers spaced 225 mm apart, and the load was applied through two load rollers centrally positioned on the specimen and spaced 75 mm apart. This assembly was installed on a testing press that loaded the specimen by lifting the lower piston at a rate of 0.40 mm *per* minute until it was no longer load-bearing. The press incorporated a load cell in the area of the upper piston and a deflection measurer in the area of the lower piston, which recorded the applied load and the deflection of the specimen at a frequency of 20 Hz. In this way, the gross load–deflection curve of the specimen was obtained.

Fifteen 75 × 75x275-mm prismatic specimens were casted for each concrete mix. They were exposed to the laboratory environment (50 ± 5% humidity and 20 ± 2 °C temperature) covered with a plastic for successful setting [5] for 1 day. After that, three specimens were subjected to the load–deflection test (concrete age of 1 day). The remaining twelve specimens were cured under two different conditions. Six of them were cured in an ambient room (60 ± 5% humidity and 20 ± 2 °C temperature) and the other six in a humid room (90 ± 5% humidity and 20 ± 2 °C temperature) to evaluate the relevance of the curing type. Three specimens exposed to each curing conditions were subjected to the load–deflection test at an age of 3 days, and another three at an age of 7 days. This organization of the experimental campaign allowed analyzing the bending behavior of concrete in a wide range of early ages and curing conditions [48].

## 2.4 Data processing

The gross load–deflection curves from the testing press were processed in several respects. Firstly, the load–deflection curves often initially show a curvature due to the settlement of the setup [7]. In reinforced concrete beams,

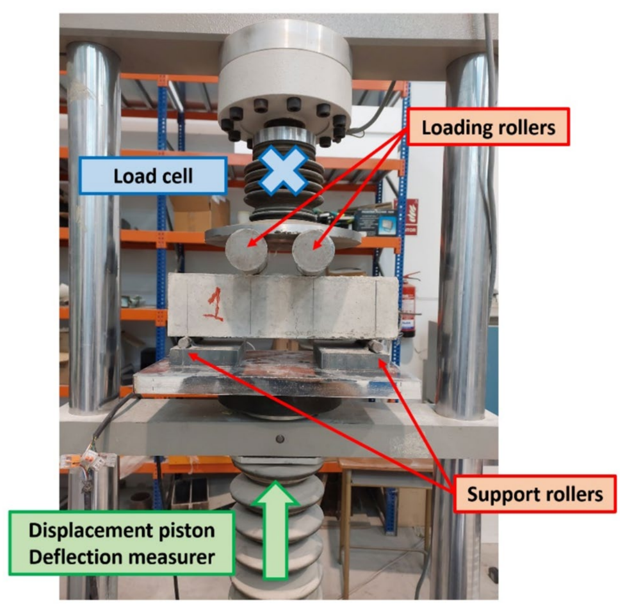


**Fig. 5** Load–deflection test setup

this problem is usually solved by applying a pre-load prior to the beginning of the test [8]. As the specimens tested in this research did not have reinforcement, the points recorded up to a deflection of 0.05 mm were removed and replaced by others that preserved the slope of the curve found for deflections between 0.05 mm and 0.10 mm, which did correspond to concrete behavior following the experience of the authors [44]. Secondly, the points with repeated load or deflection values, probably resulting from the high frequency of data collection as in other cases [8], were eliminated. Finally, the points at which the applied load was null were deleted, since the specimens did not show load-bearing capacity at these points, thus not being part of the load–deflection curve [37].

The different aspects that describe the bending behavior of concrete, schematically represented in Fig. 6, were calculated for each load–deflection curve after processing:

- The compliance shows the opposition of concrete to deflection when loaded. A lower compliance value means a lower deformability. It is defined as the inverse of the slope of the pre-failure zone of the load–deflection curve [8].
- The failure point is where the maximum load is reached [5]. This point is defined by its deflection (failure deflection) and its stress (failure stress or flexural strength).
- The fracture point is the point with the highest deflection for which the concrete is able to withstand load [38]. It is characterized by its deflection and stress values. If this point is close to the failure point, the concrete has no load-bearing capacity after failure (Fig. 6a). On the contrary, if it clearly differs from the failure point (much higher deflection and much lower load), the load-bearing capacity of concrete after failure is remarkable (Fig. 6b) [44].
- Finally, the area enclosed under the load–deflection curve represents the energy absorbed by the concrete during the bending loading process [44]. The higher this energy, the more ductile the behavior of concrete, which is essentially linked to a higher load-bearing capacity after failure [36].

## 2.5 Obtention of results and statistical analyses

Three values for each property of the load–deflection curve were obtained for each mix, concrete age, and curing conditions. Outliers were identified by applying Grubbs statistical test, which analyzes the validity of each

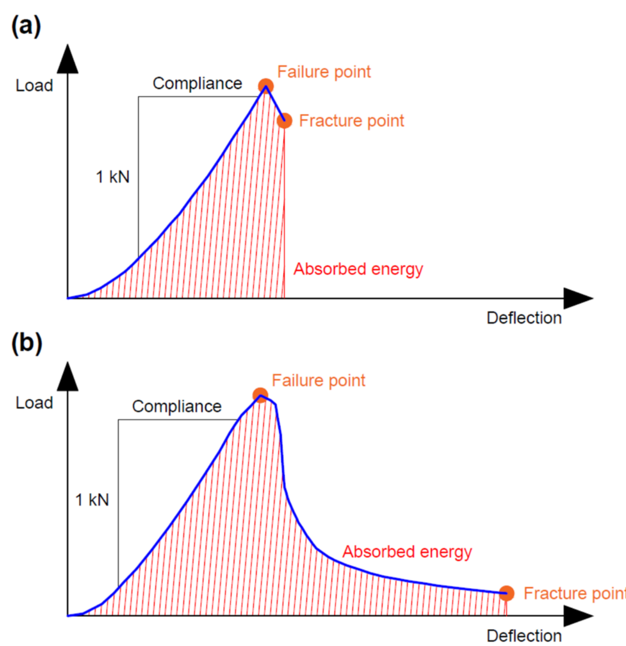


**Fig. 6** Overview of load–deflection curves in concrete: **a** without load-bearing capacity after failure; **b** with load-bearing capacity after failure

individual result by accounting for the average value and standard deviation of the whole sample of results [49]. The final values of each property for each mix, concrete age, and curing conditions, which are presented in subsequent sections, were calculated as the mean value of those results that were identified as non-outliers.

The significance of the effect of each factor (CRA amount, RCWTB content, age of concrete, and curing conditions) on the bending performance of concrete, as well as their interactions (modification of the effect of a factor when varying any or all of the other factors) were evaluated by a 95%-confidence level ANalysis Of VAriance (ANOVA), considered valid for statistical analysis in concrete research [50].

Finally, the dependencies between the different properties of the load–deflection curves were evaluated through Pearson's, Spearman's, and Kendall's correlations. These correlations show whether there is a direct (positive sign) or inverse (negative sign) dependence between two variables. Moreover, the closer their absolute value is to 1, the stronger this dependence will be. Pearson's correlations analyze the existence of linear dependence; Spearman's correlations, monotonic dependence, *i.e.*, if the variables increase or decrease simultaneously, but at different rates; and Kendall's correlations, ordinal association [51].

## 3 Results and discussion

### 3.1 Load–deflection curves

Figure 7 and Fig. 8 show all the load–deflection curves obtained in this experimental campaign for ambient and moist curing, respectively. Three specimens were tested for every mix at each age and curing condition. All of them conformed to a conventional shape, which is illustrated in Fig. 6. However, it was detected that the presence of RCWTB led to a little difference, as the curves corresponding to some mixes that incorporated RCWTB exhibited a higher initial curvature than those prepared without this waste. The higher water/cement ratios of these mixes, which reduced the stiffness of the cementitious matrix [52], as well as the presence of particles much more deformable than natural aggregate (polymers and balsa wood) [53] could have resulted in this behavior. This phenomenon was found mainly at ages of 1 and 3 days, since at older ages the cementitious matrix was more rigid and could compensate for this effect [44].

### 3.2 Compliance

The compliance represents the deformability of the mixtures before reaching the failure point, which is depicted in Fig. 9 for all the mixes in this study. All the values were within the usual range for a conventional structural concrete [5]. The compliance was lower the older the age of concrete and when a moist curing was conducted, because both factors allow for more effective hydration of concrete and, therefore, greater stiffness development [48]. The effect of age was more noticeable in this case.

CRA addition generally increased the compliance and, therefore, the bending deformability of concrete. Thus, the *0CRA/0RCWTB* mix presented a 1-day compliance of 0.0395 mm/kN, while that of the *100CRA/0RCWTB* mix was 0.0513 mm/kN (30% increment). As detailed in the literature, the bonded mortar present in the CRA makes the aggregate particles more deformable [21], leading to a decrease in the stiffness of the mix [52]. However, some of the other factors introduced in the analysis affected this general trend. On one hand, the increase in compliance with the CRA content was approximately linear in the mixes without RCWTB. However, their simultaneous use with 6% RCWTB caused the use of 100% CRA to yield concrete with a compliance always equal to or lower than that resulting from the addition of 50% CRA. For example, the *50CRA/6RCWTB* and *100CRA/6RCWTB* mixes had 1-day compliances of 0.0634 mm/kN and 0.0552 mm/kN, respectively. It is possible that the combination of such high CRA contents with the deformable particles of polymers and balsa wood contained in the RCWTB weakened the cementitious matrix, which favored cracking at lower load levels [53]. Thus, the elasticity of the cementitious matrix did not contribute as much to the pre-failure behavior [8]. On the other hand, a higher concrete

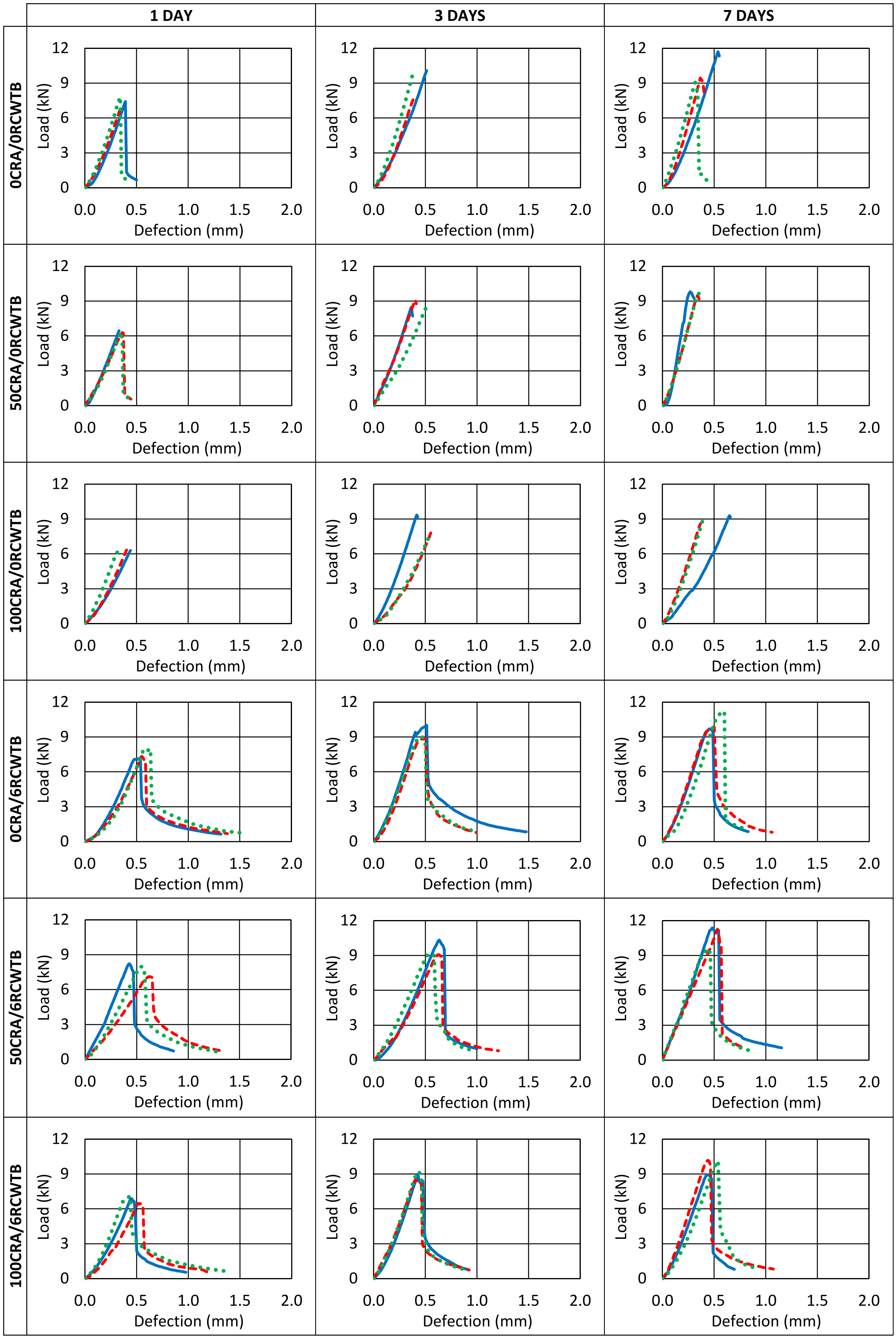


**Fig. 7** Load–deflection curves under ambient curing

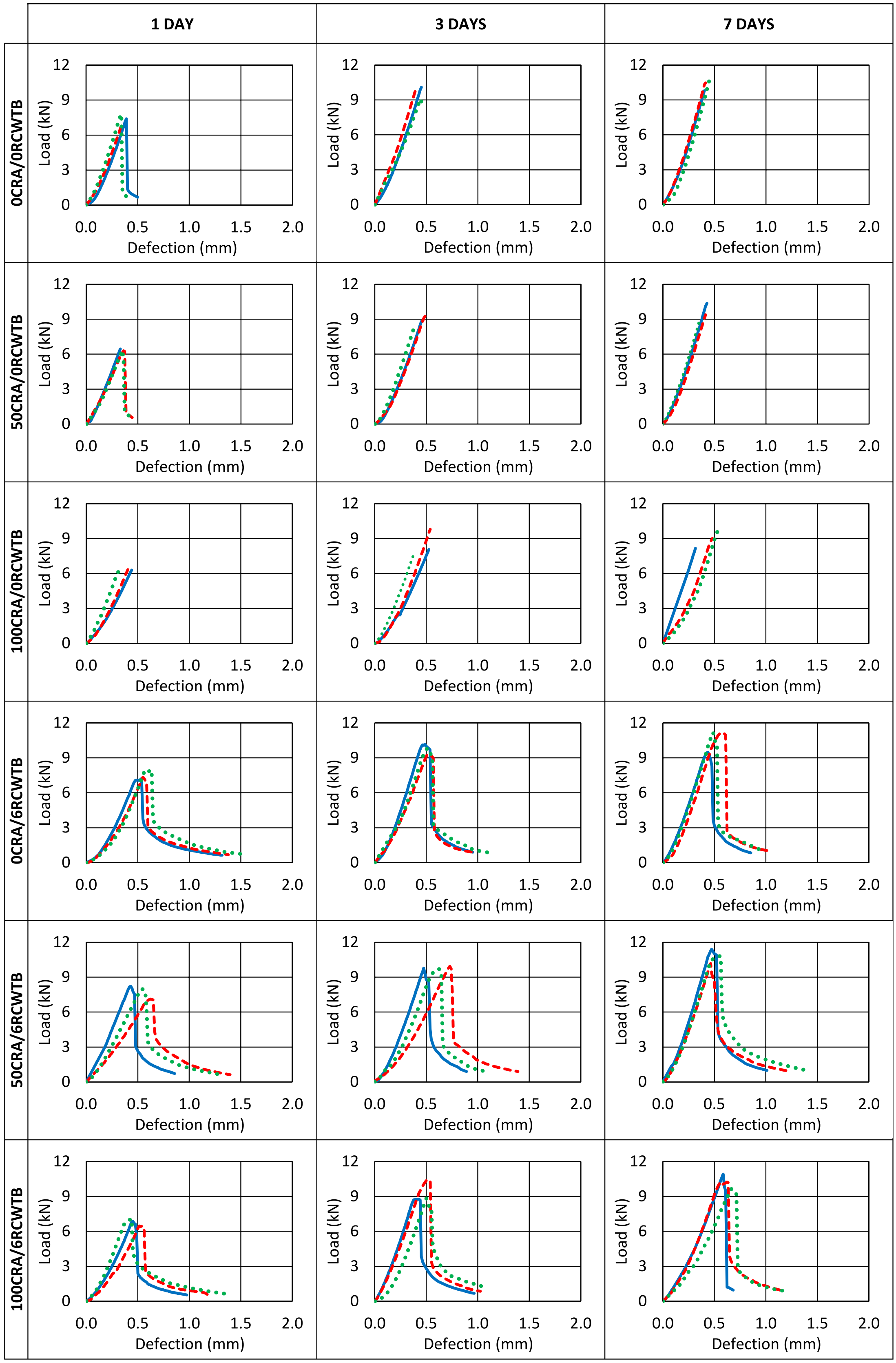


**Fig. 8** Load–deflection curves under moist curing

**Fig. 9** Compliance of the concrete mixes: **a** ambient curing; **b** moist curing

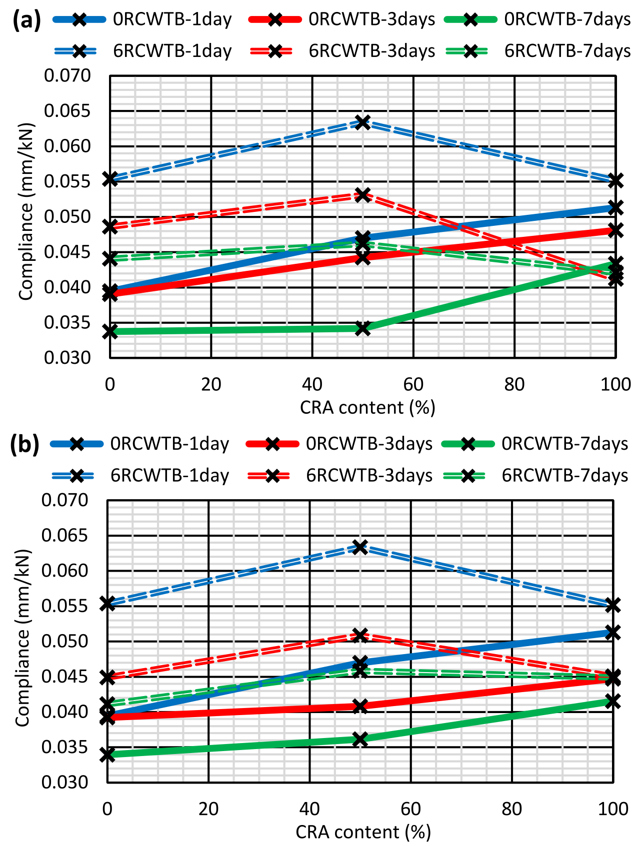


age limited the increase in compliance due to CRA addition, as it favored cement hydration [28] and, therefore, a higher matrix stiffness [18]. For example, the increase in compliance at 1 day when 50% RCA was added was 0.0075 mm/kN and 0.0080 mm/kN when combined or not with RCWTB, respectively, whereas these increases were between 0.0005 mm/kN and 0.0047 mm/kN at 7 days regardless the curing conditions. The curing environment did not affect the CRA effect on compliance.

Examining the effect of RCWTB, it can be noted that this waste generally resulted in an increased compliance. As has been found with other fiber types [27], the GFRP fibers stitched the cementitious matrix, thereby causing cracking at higher load levels, increasing the pre-failure deformability of concrete [37]. This effect was especially noteworthy when 50% CRA was combined with RCWTB because of the possible friction of the GFRP fibers with the bonded mortar of some CRA particles [54]. For example, the 1-day compliance went from 0.0395 mm/kN to 0.0554 mm/kN in mixes without CRA when RCWTB was added, and from 0.0470 mm/kN to 0.0634 mm/kN in mixes with 50% CRA. From a global approach, this trend was not modified by either the testing age or the curing conditions. However, an exception linked to the use of 100% CRA in the concrete at advanced ages was detected, since in some cases, the RCWTB reduced the compliance or, at least, kept it constant, due to the tendency of the concrete to crack when high amounts of both residues were combined, as described in the previous paragraph [53]. This phenomenon was observed mainly at an age of 3 days for ambient curing, conditions at which the compliance of the mix *100CRA/6RCWTB* was 0.0481 mm/kN, while that of the mix *100CRA/6RCWTB* was 0.0412 mm/kN.

 https://doi.org/10.1007/s43452-025-01215-5

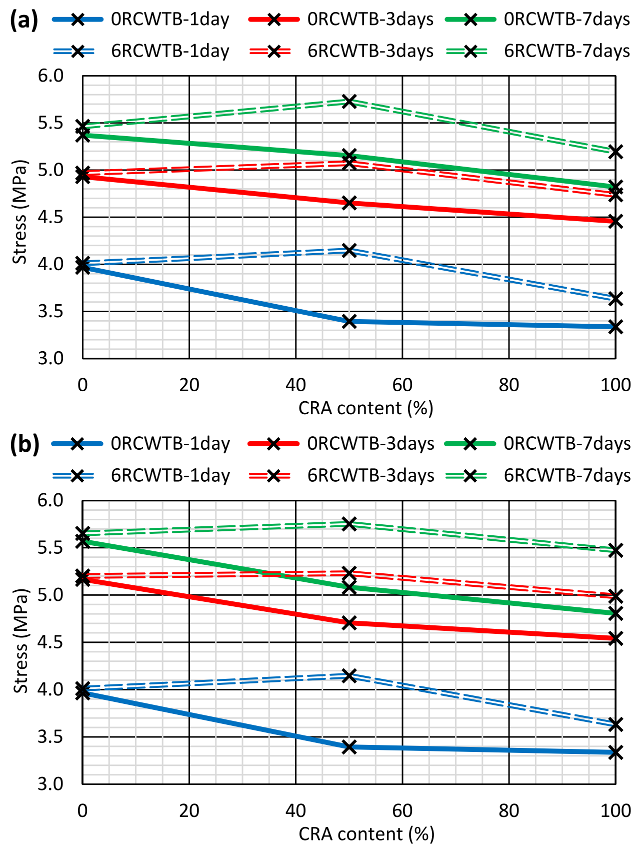


**Fig. 10** Failure stress of the concrete mixes: **a** ambient curing; **b** moist curing

## 3.3 Failure point

### 3.3.1 Failure stress

The load–deflection curves exhibited a linear behavior until the failure point, where the highest bending stress (flexural strength) was reached. All the failure stresses are depicted in Fig. 10, a detailed analysis of which can be found elsewhere [54]. The different factors analyzed affected the failure stress, but noticeable interactions were only found when simultaneously adding both residues:

- As expected from the literature [26], both advanced concrete age and moist curing always increased the failure stress regardless of the other factors due to the enhanced cement hydration they provided [48].
- The addition of CRA to concrete without RCWTB always reduced the failure stress. The bonded mortar in the CRA weakened the ITZs in the tensile-stress zone [21], feature that strongly conditions the bending performance in failure [20]. The sharpest decrease in the failure stress generally occurred at early ages when adding 50% CRA, as the decrease with the CRA amount was almost linear at an age of 7 days because the higher strength of the cementitious matrix counteracted such phenomena [55]. For instance, the decreases after 1 day of curing were 14.5% and 15.9% for 50% and 100% CRA, respectively, while these reductions were 8.7% and 13.7% after 7 days of moist curing.
- RCWTB addition always improved the failure stress compared to a mix with the same content of CRA but without RCWTB regardless of the age and curing method. Furthermore, it modified the trend caused by CRA additions. The incorporation of 50% CRA to a concrete mix with 6% RCWTB yielded a higher failure stress than that of the mix with 6% RCWTB and 0% CRA. The GFRP fibers from the RCWTB may have rubbed with some CRA particles [56], improving their stitching effect [54]. This behavior was not as efficient when RCWTB was combined with 100% CRA, since the weakening of the ITZs in those mixes was excessive due not

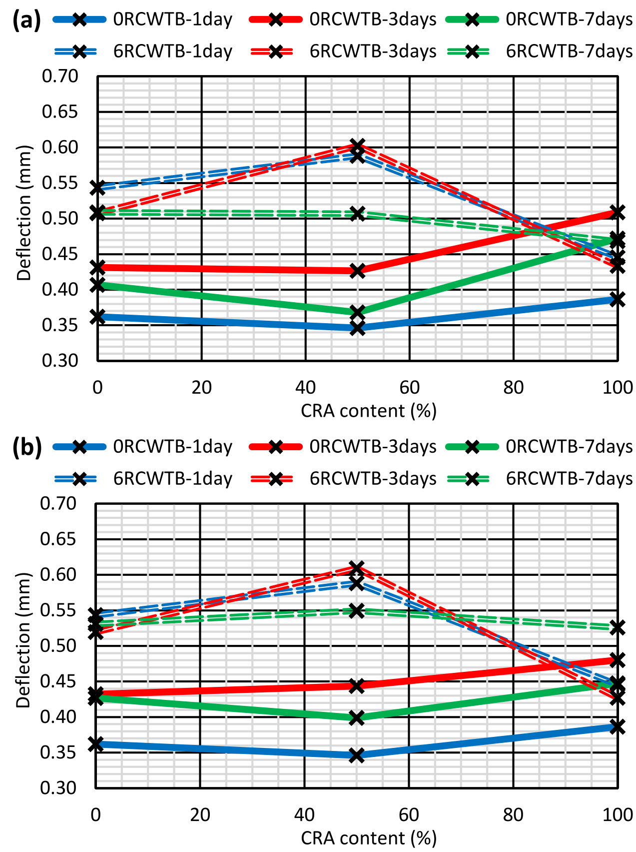


**Fig. 11** Failure deflection of the concrete mixes: **a** ambient curing; **b** moist curing

only to the high amount of CRA but also to the particles of polymers and balsa wood present in the RCWTB [53]. The *50CRA/6RCWTB* mix always exhibited the highest failure stress (5.75 MPa at 7 days).

#### 3.3.2 Failure deflection

The failure deflection was strongly conditioned by the compliance (Fig. 9) and the failure stress (Fig. 10) exhibited by the concrete mixes. In general, a higher failure deflection is linked to a higher energy-absorption capacity before failure if the failure stress is not modified [22]. The value of all the failure deflections is detailed in Fig. 11, in which it can be noted the existence of various interactions between the different factors that affected the trends displayed.

Mixes incorporating no RCWTB and with CRA contents up to 50% exhibited an approximately constant failure deflection, with variations around 2–9% in absolute value. The increase in compliance that such CRA additions caused compensated for the decrease in failure stress [57]. The failure deflection increased more noticeably (increases of 5–16%) with 100% CRA, due to the much larger increase in concrete compliance it caused [37].

The addition of RCWTB to concrete with up to 50% CRA always increased the failure deflection compared to a concrete mix of the same age and curing environment and with exactly the same composition but without RCWTB. The average increase in failure deflection caused by RCWTB under these conditions was 40% and reached a maximum value of 70% in concrete with 50% CRA at 1 day. This behavior can be explained by two aspects. First, the compliance increase caused by the stitching effect of the GFRP fibers present in the RCWTB [38]. Second, the non-modification and even enhancement of the failure stress that RCWTB provoked [54]. However, the RCWTB had a negative effect on the failure deflection of the mixtures with 100% CRA, as they showed a lower failure deflection than the mix with 0% CRA. The weak particles of polymers and balsa wood present in the blade waste resulted in a marked decrease in both compliance and failure stress, which in turn led

 https://doi.org/10.1007/s43452-025-01215-5

to a decrease in the failure deflection [58]. For instance, the 3-day failure deflection of the *100CRA/6RCWTB* mix was lower than that of the *100CRA/0RCWTB* mix (0.43 mm vs. 0.51 mm for an ambient curing, and 0.43 mm vs. 0.48 mm under moist curing).

Age also affected the failure deflection, but its effect depended on the wastes in the concrete mix. Thus, the failure deflection at 3 days was always higher than that at 7 days in the mixes without RCWTB, the deflection obtained at 1 day being the lowest of all, as a result of the changes in compliance and failure strain that concrete underwent at each age [59]. For the mixes with RCWTB, the trend was different, since the stitching effect of the GFRP fibers contained in the RCWTB produced minimal variations in failure deflection between the ages of 1 and 3 days (average variation of 2%). However, RCWTB caused that the 7-day failure deflection did not depend on the CRA content due to the improved adhesion of the GFRP fibers to the cementitious matrix [44]. The 7 day failure deflection under ambient curing was around 0.50 mm for the mixes with RCWTB regardless of the CRA amount, while it was 0.55 mm for a moist curing.

The curing environment was the factor that least affected the failure deflection of the concrete mixes, nor did it modify the individual effect of the other factors. Thus, moist curing always led to failure deflections equal to or minimally higher than ambient curing, due to the greater stiffness development of the cementitious matrix that it allowed [14].

## 3.4 Fracture point

### 3.4.1 Fracture stress

The fracture stress for the concrete mixes is detailed in Fig. 12 for both ambient curing (Fig. 12a) and moist curing (Fig. 12b). The mixes showed the same tendencies for both curing conditions, although moist curing generally

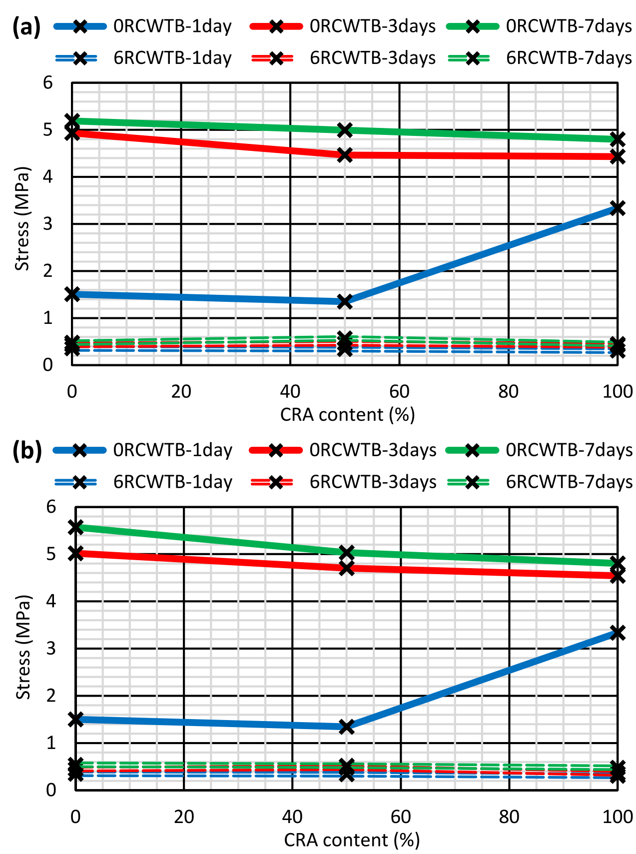


**Fig. 12** Fracture stress of the concrete mixes: **a** ambient curing; **b** moist curing

led to 2% higher fracture stresses on average. This small increase could have been due to the development of higher concrete stiffness in a wet environment [48], which resulted in a slightly more brittle fracture at the point at which the concrete was no longer capable of bearing load [44].

The bending behavior of the mixes without RCWTB depended on the age. On one hand, concrete showed a slight load-bearing capacity at 1 day and up to a CRA content of 50% due to its reduced stiffness [54]. Thus, the fracture stresses of the *0CRA/0RCWTB* and *50CRA/0RCWTB* mixes were 1.50 MPa and 1.35 MPa, respectively, while the *100CRA/0RCWTB* mix exhibited a value of 3.34 MPa. The presence of high CRA contents created ITZs of lower quality [60], which reduced the load-bearing capacity of concrete after failure. On the other, no mix without RCWTB showed load-bearing capacity at 3 and 7 days, with all fracture stresses being around 5 MPa. A more effective hydration of the cement allowed concrete to develop a higher stiffness [61], fostering a more brittle fracture [18]. CRA favored a lower stiffness development [52], which led to a decreasing fracture stress with the content of this waste at such ages. For instance, the fracture stress after 7 days of moist curing was 5.57 MPa for the *0CRA/0RCWTB* mix and 4.81 MPa for the *100CRA/0RCWTB* mix.

Concrete with 6% RCWTB exhibited a remarkable load-bearing capacity, with fracture stresses in the range of 0.3–0.6 MPa. In addition, this residue led the concrete to exhibit two marked differences compared to that without RCWTB. First, the fracture stress did not depend on the CRA content, as the variations in such property between the mixtures with 0% and 100% CRA were 0.01–0.09 MPa, thus remaining approximately constant. Second, the fracture stress was not conditioned by concrete age. Although the fracture stress increased at advanced ages, such increases were minimal, the maximum value being 0.19 MPa in the *0CRA/6RCWTB* mix. It seems clear that when RCWTB was added to concrete, its fracture stress and, therefore, its load-bearing capacity depended almost exclusively on the stitching effect of the GFRP fibers that it contained [37]. Neither the weak ITZs or the decrease in stiffness caused by CRA [60], nor the increased stiffness of the cementitious matrix with age [55] played a major role in this behavior.

**Fig. 13** Fracture deflection of the concrete mixes: **a** ambient curing; **b** moist curing

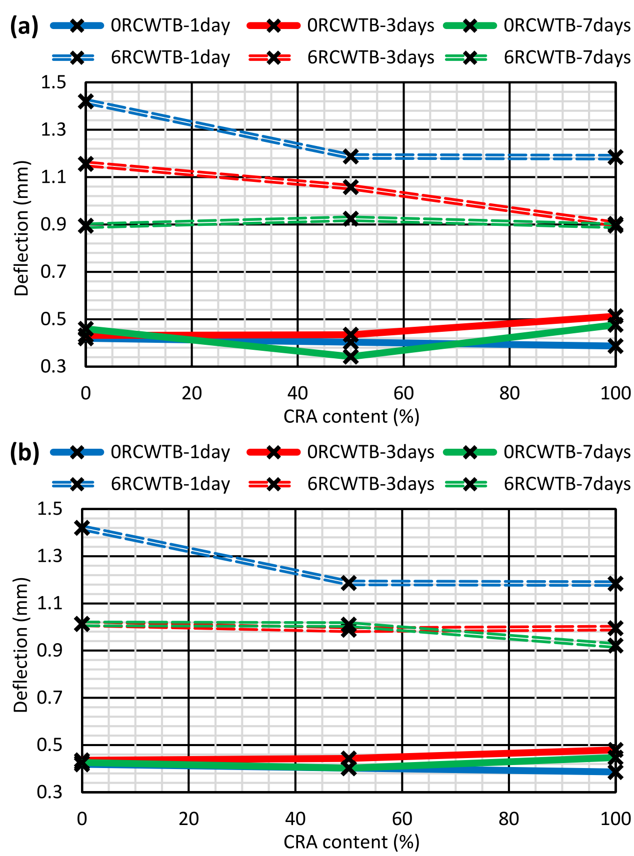

### 3.4.2 Fracture deflection

The trends shown by the fracture deflections (Fig. 13) matched the performance described for the fracture stresses. This property allowed discerning not only if concrete exhibited load-bearing capacity after failure, but also if it was relevant, *i.e.*, if it covered a wide range of deflections from the failure point [22].

The mixes without RCWTB presented low fracture deflections, in the range between 0.3 mm and 0.5 mm, values very similar to those at failure (Fig. 11). This revealed that although some of these mixtures evidenced load-bearing capacity at 1 day in terms of fracture stress (Fig. 12), this capacity was preserved over a very narrow range of deflections, not being really effective in improving the usual brittle behavior of concrete [3]. CRA addition did not cause a clear behavioral trend, the weakening of the ITZs or the decrease of the stiffness of the cementitious matrix discussed above randomly predominating [52]. Similarly, the concrete age and the curing conditions did not relevantly affect this behavior either. All these statements are based on the fact that deflections were reduced, and variations were minimal compared to the values achieved in the RCWTB mixes.

Mixes with RCWTB showed much higher fracture deflections, with a minimum value of 0.90 mm (*100CRA/6RCWTB* mix at 7 days under ambient curing) and reaching values of up to 1.42 mm (*0CRA/6RCWTB* mix at 1 day). All the mixtures made with this residue showed a remarkable load-bearing capacity [37], regardless of the other factors. However, these factors did affect the fracture deflection obtained:

- First, increasing CRA amounts reduced the fracture-deflection improvement when RCWTB was added because of the weakening of the ITZs that this alternative aggregate caused [60]. For example, the decrease in fracture deflection from 0 to 100% CRA was 16.6% at 1 day. Moreover, this decrease was conditioned by the concrete age, since the decrease due to CRA addition was more noticeable at early ages, becoming almost negligible at 7 days of ambient curing (Fig. 13a). The higher strength at advanced ages of the cementitious matrix favored a higher bond in the ITZs [46].
- Second, the increase in failure deflection resulting from RCWTB addition was more marked at earlier ages. For instance, the failure deflections of the *50CRA/6RCWTB* mix under ambient curing were 1.19 mm, 1.06 mm, and 0.92 mm at 1, 3, and 7 days, respectively. The higher cement hydration and, therefore, stiffness development of the cementitious matrix with age promoted a more brittle fracture and lower deflection levels [57]. In addition, this behavior was conditioned by the curing type, since moist curing led the fracture deflection at 3 days and 7 days to be the same regardless of the CRA content. A wet environment favored the cementitious matrix to develop a more notable stiffness at early ages [48].

## 3.5 Absorbed energy

The values of the energy absorbed by the mixtures during bending loading are detailed in Fig. 14. The definition of absorbed energy (Fig. 6) shows that this feature was conditioned by the trends exhibited by the rest of the load–deflection properties [44].

First, it is noteworthy that concrete made with RCWTB always showed higher absorbed energy than concrete without such residue regardless of the CRA content of the concrete, its age, and its curing conditions. The GFRP fibers stitched the cementitious matrix, generally increasing compliance, failure strain and, most importantly, providing load-bearing capacity after failure, as exposed in previous sections. These factors in turn led to an increase in the area enclosed under the load–deflection curve [37]. For example, the increase in 7-day absorbed energy of the *50CRA/6RCWTB* mix with respect to the *50CRA/0RCWTB* mix was around 135%. This behavior is similar to that exhibited by other types of fibers [22] and shows the validity of RCWTB to improve the energy absorption of concrete with CRA in all cases.

**Fig. 14** Energy absorbed by the concrete mixes: **a** ambient curing; **b** moist curing

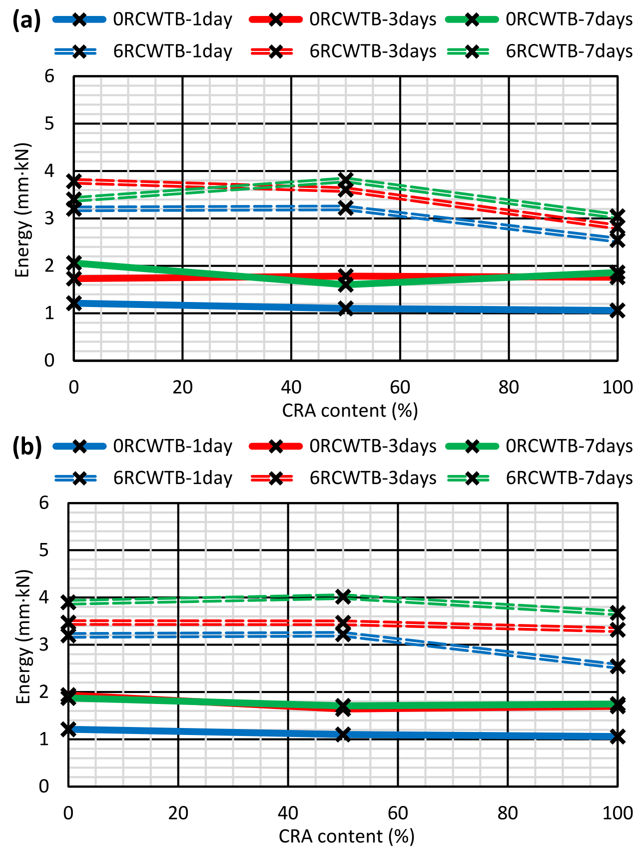


The absorbed energy was also affected by the CRA content, although its effect was different depending on whether or not it was combined with RCWTB:

- On the one hand, the absorbed energy of concrete without RCWTB was not affected by the CRA content and remained approximately constant for any age and curing condition. As explained in previous sections, this alternative aggregate increased the compliance and reduced the failure strain in the absence of RCWTB, while it did not improve concrete load-bearing capacity. The reduced bond between the cementitious matrix and the CRA in the ITZs and the high flexibility of this aggregate justify such behaviors [60]. Thus, both properties compensated each other's effect, which led the area under the load–deflection curve to experience minimal variations [57]. The absorbed energy for all mixes without RCWTB was between 1 and 2 mm·kN.
- On the other hand, the addition of up to 50% CRA to concrete with RCWTB did not affect the absorbed energy due to the optimal interaction of RCWTB with such CRA content, which resulted in an increase in the concrete's failure strain [54]. However, the use of 100% CRA reduced the compliance and failure strain because of the features discussed above for concrete without RCWTB, which also notably decreased the absorbed energy. For example, the 1-day absorbed energies for concrete containing 6% RCWTB were 3.20 mm·kN, 3.22 mm·kN, and 2.55 mm·kN for 0%, 50%, and 100% CRA contents, respectively. The decrease caused by 100% CRA was more noticeable for 1-day age and ambient curing, since for them the ITZs were less stiff and strong [48].

Finally, it should be noted that the absorbed energy increased with age, but only up to 3 days, so that the absorbed-energy levels of concrete at 3 and 7 days were the same. The only exception was encountered in mixes incorporating RCWTB when subjected to moist curing, where at 7 days the energy absorbed was

**Table 3** *P*-values for the factors

| Property | CRA amount (factor A) | RCWTB amount (factor B) | Age (factor C) | Curing (factor D) |
|---|---|---|---|---|
| Compliance | 0.0000 | 0.0000 | 0.0000 | 0.1469 |
| Failure stress | 0.0000 | 0.0000 | 0.0000 | 0.0098 |
| Failure deflection | 0.0000 | 0.0000 | 0.0000 | 0.0562 |
| Fracture stress | 0.0000 | 0.0000 | 0.0000 | 0.1423 |
| Fracture deflection | 0.0000 | 0.0000 | 0.0000 | 0.1286 |
| Absorbed energy | 0.0000 | 0.0000 | 0.0000 | 0.0556 |

**Table 4** *P*-values for the second-order interactions

| Property | A–B | A–C | A–D | B–C | B–D | C–D |
|---|---|---|---|---|---|---|
| Compliance | 0.0000 | 0.0000 | 0.2779 | 0.0000 | 0.5382 | 0.1406 |
| Failure stress | 0.0000 | 0.5483 | 0.3700 | 0.3470 | 0.2908 | 0.1243 |
| Failure deflection | 0.0000 | 0.0000 | 0.1474 | 0.0000 | 0.0535 | 0.0653 |
| Fracture stress | 0.0000 | 0.0000 | 0.6400 | 0.0000 | 0.1666 | 0.5716 |
| Fracture deflection | 0.0000 | 0.0000 | 0.0673 | 0.0000 | 0.0849 | 0.0000 |
| Absorbed energy | 0.0000 | 0.0332 | 0.0448 | 0.0792 | 0.0530 | 0.0429 |

10–16% higher than at 3 days. As found in other studies, wet curing favored a more effective hydration of the cementitious matrix [9], and thus a better bond with the fibers [25], which improved their stitching effect and, therefore, allowed a slightly higher ductility of the concrete [38].

### 3.6 Statistical significance

The effects of four factors (CRA content, RCWTB amount, age, and curing environment) on the load–deflection performance of concrete have been evaluated in this research. The significance of their effect on concrete behavior was therefore statistically validated by means of a four-way ANOVA at 95% confidence level that included all the non-outlier individual experimental values, as usually conducted in concrete research [50]. Table 3 shows the *p*-values referring to each factor significance, while Table 4 enumerates the *p*-values corresponding to the significance of the second-order interactions. *P*-values less than 0.05 indicated that either the factor or the interaction was significant. All the third-order interactions were non-significant.

Regarding the factors (Table 3), both CRA and RCWTB contents and age significantly affected all the load–deflection properties of concrete. Moreover, their significance was high because the *p*-values were far from the reference value of 0.05. The only exception was the factor "curing conditions", which did not significantly affect the concrete performance except in terms of failure stress. Curing the concrete in a moist environment favors a more effective cement hydration, but this aspect often becomes more noticeable at older ages [48]. In addition, the high water-absorption levels of CRA can alleviate this effect in the short term by this aggregate type providing an internal curing effect [62].

Second-order interactions, whose *p*-values are detailed in Table 4, show if the effect of a factor is different for each value adopted by the rest of the factors [51]. There were three interactions whose significance was recurrent. First, the interaction between the RCWTB and CRA amounts was always significant. As detailed for all properties, the effect of CRA was different depending on whether or not it was combined with RCWTB in concrete, as the adherence of the GFRP fibers was improved by certain CRA amounts [54]. Second, the interaction between the CRA amount and the concrete age, which was not significant only for the failure stress. The reduced stiffness and bond in the ITZs caused by this alternative aggregate was more pronounced at early ages [21]. Finally, the interaction between the RCWTB content and the concrete age. An older concrete age allowed a higher bond to the cementitious matrix of the GFRP fibers of the RCWTB, favoring a more relevant stitching effect [25]. The

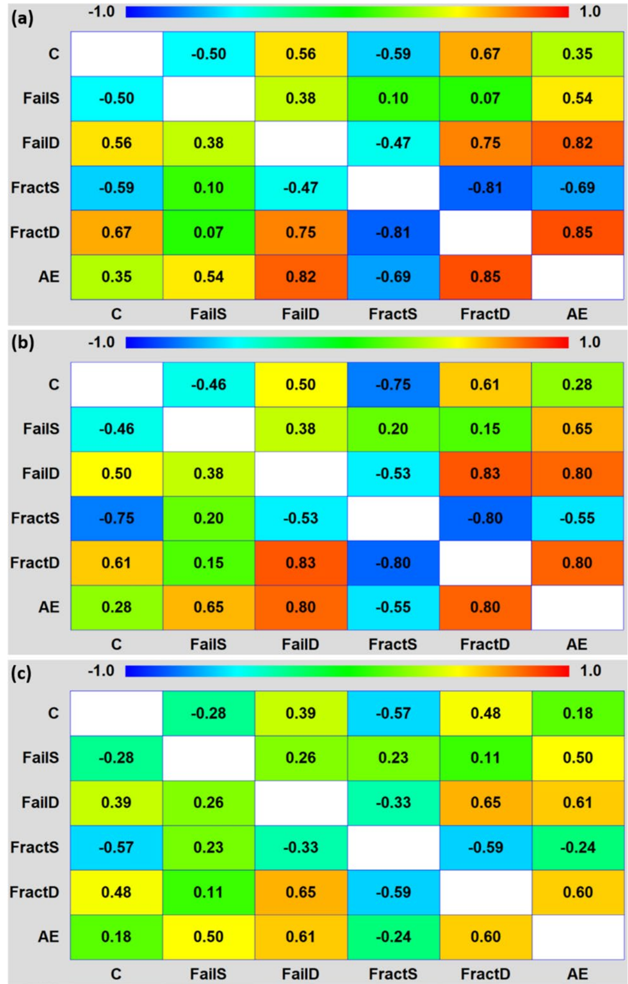


**Fig. 15** Correlations between the load–deflection properties of the concrete mixes: **a** Pearson; **b** Spearman; **c** Kendall (legend: *C*, compliance; *FailS*, failure stress; *FailD*, failure deflection; *FractS*, fracture stress; *FractD*, fracture deflection; *AE*, absorbed energy)

rest of the second-order interactions were only significant in specific cases, not affecting the overall behavior of the concrete under bending.

### 3.7 Correlation analysis

To conclude the study, a correlation analysis was conducted between the different load–deflection properties of the mixes to elucidate the existing relationships between them. The correlation matrices are shown in Fig. 15, considering as relevant those with an absolute value equal to or greater than 0.75 [51]. The ordinal association reflected by the Kendall's correlations (Fig. 15c) was low, *i.e.*, the highest values of all the properties did not always correspond to the same mixtures.

From the analysis of the Pearson's (Fig. 15a) and Spearman's (Fig. 15b) correlations, three aspects stand out as relevant:

- First, there was an inverse monotonic correlation (Spearman's correlations, Fig. 15b) between the compliance and the fracture stress. The addition of RCWTB decreased the pre-failure stiffness of concrete, the concrete also exhibiting a lower fracture stress and a higher load-bearing capacity. RCWTB augmented the deformability of concrete both before and after failure thanks to the stitching effect of the GFRP fibers [42].
- Second, fracture deflection showed two relevant correlations, monotonic with the failure deflection (Spearman's correlations, Fig. 15b) and linear with the fracture stress (Pearson's correlations, Fig. 15a). A higher

load-bearing capacity of concrete implies a larger fracture deflection [44], and it was increased when the deformability at the failure point was higher and the lower the stress up to which concrete was able to bear load after failure. This performance has also been found with other types of fibers [4] and shows that both failure and post-failure behaviors are relevant in terms of the concrete load-bearing capacity [22].

- Finally, the absorbed energy was significantly conditioned by both the failure and fracture deflections (Pearson's correlations, Fig. 15a). The improvement caused by RCWTB in the absorbed energy was mainly due to the increase in deflection terms, being the pre-failure stiffness relegated to a secondary role, as noted for other types of concrete fibers [8].

## 4 Conclusions

In this study, the bending behavior at an early age of concrete made simultaneously with Raw-Crushed Wind-Turbine Blade (RCWTB) and Coarse Recycled Aggregate (CRA) has been analyzed. The load–deflection curves of concrete mixes prepared with 0%, 50% and 100% CRA and 0% and 6% RCWTB have been characterized in terms of deformability, stress and energy absorption at three different ages (1, 3 and 7 days) and under both ambient and moist curing. The following conclusions can be drawn:

- RCWTB increased concrete compliance, as the fibers of Glass Fiber-Reinforced Polymer (GFRP) it contained caused that the beginning of concrete cracking occurred at higher load levels. This was particularly noticeable when combined with 50% CRA, as this CRA amount weakened the stiffness of concrete to a lesser extent. The negative effect of CRA was less relevant at older concrete ages.
- The decrease in failure stress caused by increasing amounts of CRA was compensated by 6% RCWTB up to 50% CRA. RCWTB even caused that concrete with such CRA content had a higher failure strain than the 0%-CRA concrete, especially at early ages and for an ambient curing, which favor a weaker cementitious matrix. Similarly, RCWTB increased the failure deflection for any CRA content, increasing concrete deformability. This effect was also especially notable for CRA amounts up to 50%.
- The load-bearing capacity of concrete after failure was always greatly improved with the use of RCWTB. In addition, CRA did not condition such behavior at advanced ages (7 days). However, a negative effect of CRA was perceived at earlier ages, as the increase in the content of this aggregate always resulted in a significant decrease of the fracture deflection regardless of RCWTB use.
- The absorbed energy of the mixes containing RCWTB, calculated as the area under the load–deflection curve, was approximately twice that of mixes with identical composition but without RCWTB. Furthermore, this residue ensured that the energy absorbed was unaffected by the use of up to 50% CRA, independently of age and curing environment. The decrease in absorbed energy when 100% CRA was used was also minimal when combined with RCWTB.
- Both CRA and RCWTB content and concrete age significantly affected the bending performance of concrete. Moreover, the interactions between them were always statistically significant, which confirmed that RCWTB performed better when combined with 50% CRA and that the stitching effect of GFRP fibers was better at advanced ages due to their better adhesion to the cementitious matrix.

Overall, RCWTB improved the bending behavior of concrete with CRA at early ages, the increase in absorbed energy being based mainly on the improvement in terms of deflection that it generated according to a correlation analysis. Therefore, it is demonstrated the feasibility of the joint use of both wastes for the manufacture of concrete to be used in elements that work in bending and that even have to be put into service at an early age under any curing type, such as building beams or pavements. These findings open a potential avenue for the simultaneous recycling of both wastes by using them as raw materials in concrete production for such kind of applications.

**Funding** Open access funding provided by FEDER European Funds and the Junta de Castilla y León under the Research and Innovation Strategy for Smart Specialization (RIS3) of Castilla y León 2021-2027. This research work was supported by the Spanish Ministry of Universities, MICINN, AEI, EU, ERDF and NextGenerationEU/PRTR [grant numbers PID2023-146642OB-I00;https://doi.org/10.13039/501100011033; TED2021-129715B-I00]; the Junta de Castilla y León (Regional Government) and ERDF [grant number UIC-231; BU033P23]; and, finally, the University of Burgos [grant number SUCONS, Y135.GI].

**Data availability** The authors declare that the data supporting the findings of this study are available within the paper. The authors are available for further clarifications.

## Declarations

**Conflict of interest** The authors declare that they have no known competing financial interests or personal relationships that could have appeared to influence the work reported in this paper.



## References

1. Alzoubi H, Elsanadedy H, Abbas H, Almusallam T, Abadel A, Al-Salloum Y. Investigating the performance of basalt FRP-reinforced concrete columns: experimental and analytical insights. Arch Civ Mech Eng. 2024;24(4):216. https://doi.org/10.1007/s43452-024-01023-3.
2. Toska K, Hofer L, Faleschini F, Zanini MA, Pellegrino C. Seismic behavior of damaged RC columns repaired with FRCM composites. Eng Struct. 2022;262: 114339. https://doi.org/10.1016/j.engstruct.2022.114339.
3. Velay-Lizancos M, Vazquez-Burgo P, Restrepo D, Martinez-Lage I. Effect of fine and coarse recycled concrete aggregate on the mechanical behavior of precast reinforced beams: comparison of FE simulations, theoretical, and experimental results on real scale beams. Constr Build Mater. 2018;191:1109–19. https://doi.org/10.1016/j.conbuildmat.2018.10.075.
4. Fang M, Chen Y, Deng Y, Wang Z, Zhu M. Toughness improvement mechanism and evaluation of cement concrete for road pavement: a review. J Road Eng. 2023;3(2):125–40. https://doi.org/10.1016/j.jreng.2023.01.005.
5. EC-2. Eurocode 2: Design of concrete structures. Part 1–1: general rules and rules for buildings. CEN (European Committee for Standardization). 2010.
6. Rincon LF, Moscoso YM, Hamami AEA, Matos JC, Bastidas-Arteaga E. Degradation models and maintenance strategies for reinforced concrete structures in coastal environments under climate change: a review. Buildings. 2024;14(3):562. https://doi.org/10.3390/buildings14030562.
7. Malumbela G, Alexander M, Moyo P. Steel corrosion on RC structures under sustained service loads - a critical review. Eng Struct. 2009;31(11):2518–25. https://doi.org/10.1016/j.engstruct.2009.07.016.
8. Santamaría A, Romera JM, Marcos I, Revilla-Cuesta V, Ortega-López V. Shear strength assessment of reinforced concrete components containing EAF steel slag aggregates. J Build Eng. 2022;46: 103730. https://doi.org/10.1016/j.jobe.2021.103730.
9. Liu B, Ye H, Jiang J, Shi J, Yalçınkaya Ç, Šavija B. Assessment of self-healing behavior of polypropylene fiber-reinforced cement mortar with crystalline admixture: the effects of crack widths, cracking ages, and external conditions. J Sustain Cem Based Mater. 2024;13(5):706–25. https://doi.org/10.1080/21650373.2023.2300996.
10. Sabbrojjaman M, Liu Y, Tafsirojjaman T. A comparative review on the utilisation of recycled waste glass, ceramic and rubber as fine aggregate on high performance concrete: mechanical and durability properties. Dev Built Environ. 2024;17: 100371. https://doi.org/10.1016/j.dibe.2024.100371.
11. Bulatbekova D, Vashistha P, Kim HK, Pyo S. Effects of basic-oxygen furnace, electric-arc furnace, and ladle furnace slags on the hydration and durability properties of construction materials: a review. J Build Eng. 2024;92: 109670. https://doi.org/10.1016/j.jobe.2024.109670.

12. Tudu C, Mohanty M, Mohapatra SS, Nayak S. A systematic review exploring the feasibility of waste plastic as different constituents towards sustainable concrete. Constr Build Mater. 2024;428: 136210. https://doi.org/10.1016/j.conbuildmat.2024.136210.
13. Hasheminezhad A, King D, Ceylan H, Kim S. Comparative life cycle assessment of natural and recycled aggregate concrete: a review. Sci Total Environ. 2024;950: 175310. https://doi.org/10.1016/j.scitotenv.2024.175310.
14. Velay-Lizancos M, Martinez-Lage I, Azenha M, Granja J, Vazquez-Burgo P. Concrete with fine and coarse recycled aggregates: E-modulus evolution, compressive strength and non-destructive testing at early ages. Constr Build Mater. 2018;193:323–31. https://doi.org/10.1016/j.conbuildmat.2018.10.209.
15. Evangelista L, de Brito J. Mechanical behaviour of concrete made with fine recycled concrete aggregates. Cem Concr Compos. 2007;29(5):397–401. https://doi.org/10.1016/j.cemconcomp.2006.12.004.
16. Xu JJ, Zhao XY, Chen ZP, Liu JC, Xue JY, Elchalakani M. Novel prediction models for composite elastic modulus of circular recycled aggregate concrete-filled steel tubes. Thin-Walled Struct. 2019;144: 106317. https://doi.org/10.1016/j.tws.2019.106317.
17. Gao S, Guo J, Zhu Y, Jin Z. Study on the influence of the properties of interfacial transition zones on the performance of recycled aggregate concrete. Constr Build Mater. 2023;408: 133592. https://doi.org/10.1016/j.conbuildmat.2023.133592.
18. Revilla-Cuesta V, Skaf M, Santamaría A, Ortega-López V, Manso JM. Assessment of longitudinal and transversal plastic behavior of recycled aggregate self-compacting concrete: a two-way study. Constr Build Mater. 2021;292: 123426. https://doi.org/10.1016/j.conbuildmat.2021.123426.
19. Silva RV, de Brito J, Dhir RK. Fresh-state performance of recycled aggregate concrete: a review. Constr Build Mater. 2018;178:19–31. https://doi.org/10.1016/j.conbuildmat.2018.05.149.
20. Revilla-Cuesta V, Faleschini F, Zanini MA, Skaf M, Ortega-López V. Porosity-based models for estimating the mechanical properties of self-compacting concrete with coarse and fine recycled concrete aggregate. J Build Eng. 2021;44: 103425. https://doi.org/10.1016/j.jobe.2021.103425.
21. Muhammad F, Harun M, Ahmed A, Kabir N, Khalid HR, Hanif A. Influence of bonded mortar on recycled aggregate concrete properties: a review. Constr Build Mater. 2024;432: 136564. https://doi.org/10.1016/j.conbuildmat.2024.136564.
22. El-Abbasy AA. Tensile, flexural, impact strength, and fracture properties of ultra-high-performance fiber-reinforced concrete – a comprehensive review. Constr Build Mater. 2023;408: 133621. https://doi.org/10.1016/j.conbuildmat.2023.133621.
23. Li Y, Chen P, Chen Z, Liu X, Liu Z, Liu Y. Influence of fiber on the shrinkage performance of alkali-activated slag recycled concrete. Arch Civ Mech Eng. 2024;24(3):153. https://doi.org/10.1007/s43452-024-00966-x.
24. Lai D, Demartino C, Xiao Y. High-strain rate tension behavior of fiber-reinforced rubberized concrete. Cem Concr Compos. 2022;131: 104554. https://doi.org/10.1016/j.cemconcomp.2022.104554.
25. Aghajanian A, Cimentada A, Behfarnia K, Brand AS, Thomas C. Microstructural analysis of siderurgical aggregate concrete reinforced with fibers. J Build Eng. 2023;64: 105543. https://doi.org/10.1016/j.jobe.2022.105543.
26. Chen L, Chen Z, Xie Z, Wei L, Hua J, Huang L, et al. Recent developments on natural fiber concrete: a review of properties, sustainability, applications, barriers, and opportunities. Dev Built Environ. 2023;16: 100255. https://doi.org/10.1016/j.dibe.2023.100255.
27. Manso-Morato J, Hurtado-Alonso N, Revilla-Cuesta V, Skaf M, Ortega-López V. Fiber-reinforced concrete and its life cycle assessment: a systematic review. J Build Eng. 2024;94: 110062. https://doi.org/10.1016/j.jobe.2024.110062.
28. Zhang X, Zhu Y, Shen Y, Wang J, Fan Y, Gao X, et al. Compressive mechanical performance and microscopic mechanism of basalt fiber-reinforced recycled aggregate concrete after elevated temperature exposure. J Build Eng. 2024;96: 110647. https://doi.org/10.1016/j.jobe.2024.110647.
29. Zhang F, Lu Z, Wang D. Working and mechanical properties of waste glass fiber reinforced self-compacting recycled concrete. Constr Build Mater. 2024;439: 137172. https://doi.org/10.1016/j.conbuildmat.2024.137172.
30. Valizadeh Kiamahalleh M, Gholampour A, Ngo TD, Ozbakkaloglu T. Mechanical, durability and microstructural properties of waste-based concrete reinforced with sugarcane fiber. Structures. 2024;67: 107019. https://doi.org/10.1016/j.istruc.2024.107019.
31. Sachin EK, Muthu N, Tiwari P. Hybrid recycling methods for fiber reinforced polymer composites: a review. J Reinf Plast Compos. 2024. https://doi.org/10.1177/07316844241258557.
32. Podara C, Termine S, Modestou M, Semitekolos D, Tsirogiannis C, Karamitrou M, et al. Recent trends of recycling and upcycling of polymers and composites: a comprehensive review. Recycling. 2024;9(3):37. https://doi.org/10.3390/recycling9030037.
33. Shen Y, Apraku SE, Zhu Y. Recycling and recovery of fiber-reinforced polymer composites for end-of-life wind turbine blade management. Green Chem. 2023;25(23):9644–58. https://doi.org/10.1039/d3gc03479h.
34. Wei Y, Hadigheh SA. Enhancing carbon fibre recovery through optimised thermal recycling: kinetic analysis and operational parameter investigation. Mater Today Sustain. 2024;25: 100661. https://doi.org/10.1016/j.mtsust.2023.100661.
35. Fonte R, Xydis G. Wind turbine blade recycling: an evaluation of the European market potential for recycled composite materials. J Environ Manage. 2021;287: 112269. https://doi.org/10.1016/j.jenvman.2021.112269.

36. Tao Y, Hadigheh SA, Wei Y. Recycling of glass fibre reinforced polymer (GFRP) composite wastes in concrete: a critical review and cost benefit analysis. Structures. 2023;53:1540–56. https://doi.org/10.1016/j.istruc.2023.05.018.
37. Xu GT, Liu MJ, Xiang Y, Fu B. Valorization of macro fibers recycled from decommissioned turbine blades as discrete reinforcement in concrete. J Clean Prod. 2022;379: 134550. https://doi.org/10.1016/j.jclepro.2022.134550.
38. Fu B, Xu GT, Peng WS, Huang JZ, Zou QQ, Kuang YD. Performance enhancement of recycled coarse aggregate concrete by incorporating with macro fibers processed from waste GFRP. Constr Build Mater. 2024;411: 134166. https://doi.org/10.1016/j.conbuildmat.2023.134166.
39. Xu MX, Ji HW, Wu YC, Meng XX, Di JY, Yang J, et al. Recovering glass fibers from waste wind turbine blades: recycling methods, fiber properties, and potential utilization. Renew Sustain Energy Rev. 2024;202: 114690. https://doi.org/10.1016/j.rser.2024.114690.
40. Joustra J, Flipsen B, Balkenende R. Structural reuse of wind turbine blades through segmentation. Compos Part C Open Access. 2021;5: 100137. https://doi.org/10.1016/j.jcomc.2021.100137.
41. Rani M, Choudhary P, Krishnan V, Zafar S. A review on recycling and reuse methods for carbon fiber/glass fiber composites waste from wind turbine blades. Compos Part B Eng. 2021;215: 108768. https://doi.org/10.1016/j.compositesb.2021.108768.
42. Baturkin D, Hisseine OA, Masmoudi R, Tagnit-Hamou A, Massicotte L. Valorization of recycled FRP materials from wind turbine blades in concrete. Resour Conserv Recycl. 2021;174: 105807. https://doi.org/10.1016/j.resconrec.2021.105807.
43. Revilla-Cuesta V, Skaf M, Ortega-López V, Manso JM. Raw-crushed wind-turbine blade: Waste characterization and suitability for use in concrete production. Resour Conserv Recycl. 2023;198: 107160. https://doi.org/10.1016/j.resconrec.2023.107160.
44. Ortega-López V, Faleschini F, Hurtado-Alonso N, Manso-Morato J, Revilla-Cuesta V. Analysis of raw-crushed wind-turbine blade as an overall concrete addition: stress–strain and deflection performance effects. Compos Struct. 2024;340: 118170. https://doi.org/10.1016/j.compstruct.2024.118170.
45. EN-Euronorm. Rue de stassart, 36. Belgium-1050 Brussels, European Committee for Standardization.
46. Luo H, Aguiar J, Wan X, Wang Y, Cunha S, Jia Z. Application of aggregates from construction and demolition wastes in concrete: review. Sustainability. 2024;16(10):4277. https://doi.org/10.3390/su16104277.
47. ASTM. Annual book of ASTM standards. 2023.
48. Sidhu AS, Siddique R. Review on effect of curing methods on high strength concrete. Constr Build Mater. 2024;438: 136858. https://doi.org/10.1016/j.conbuildmat.2024.136858.
49. Vivekanandan N. Assessment of uncertainty in estimation of rainfall using EV1 distribution with reference to data length. Mausam. 2024;75(3):801–14. https://doi.org/10.54302/mausam.v75i3.6236.
50. Cantero B, Bravo M, de Brito J, Sáez del Bosque IF, Medina C. Mechanical behaviour of structural concrete with ground recycled concrete cement and mixed recycled aggregate. J Clean Prod. 2020;275:122913. https://doi.org/10.1016/j.jclepro.2020.122913.
51. Revilla-Cuesta V, Serrano-López R, Espinosa AB, Ortega-López V, Skaf M. Analyzing the relationship between compressive strength and modulus of elasticity in concrete with ladle furnace slag. Buildings. 2023;13(12):3100. https://doi.org/10.3390/buildings13123100.
52. Silva RV, De Brito J, Dhir RK. Establishing a relationship between modulus of elasticity and compressive strength of recycled aggregate concrete. J Clean Prod. 2016;112:2171–86. https://doi.org/10.1016/j.jclepro.2015.10.064.
53. Islam MJ, Shahjalal M, Haque NMA. Mechanical and durability properties of concrete with recycled polypropylene waste plastic as a partial replacement of coarse aggregate. J Build Eng. 2022;54: 104597. https://doi.org/10.1016/j.jobe.2022.104597.
54. Trento D, Faleschini F, Revilla-Cuesta V, Ortega-López V. Improving the early-age behavior of concrete containing coarse recycled aggregate with raw-crushed wind-turbine blade. J Build Eng. 2024;92: 109815. https://doi.org/10.1016/j.jobe.2024.109815.
55. Vintimilla C, Etxeberria M, Li Z. Durable structural concrete produced with coarse and fine recycled aggregates using different cement types. Sustainability. 2023;15(19):14272. https://doi.org/10.3390/su151914272.
56. García-González J, Rodríguez-Robles D, Wang J, De Belie N, Morán-del Pozo JM, Guerra-Romero MI, et al. Quality improvement of mixed and ceramic recycled aggregates by biodeposition of calcium carbonate. Constr Build Mater. 2017;154:1015–23. https://doi.org/10.1016/j.conbuildmat.2017.08.039.
57. Revilla-Cuesta V, Ortega-López V, Skaf M, Khan AUR, Manso JM. Deformational behavior of self-compacting concrete containing recycled aggregate, slag cement and green powders under compression and bending: Description and prediction adjustment. J Build Eng. 2022;54: 104611. https://doi.org/10.1016/j.jobe.2022.104611.
58. Jang ES, Kang CW. Porosity analysis of three types of balsa (Ochroma pyramidale) wood depending on density. J Wood Sci. 2022;68(1):31. https://doi.org/10.1186/s10086-022-02037-2.
59. Fu B, Lin LB, Zhou X, You XM, Deng DY. Effect of incorporating recycled macro fibres on the properties of ultra-high-performance seawater sea-sand concrete. J Build Eng. 2024;83: 108460. https://doi.org/10.1016/j.jobe.2024.108460.

60. Guedes M, Evangelista L, De Brito J, Ferro AC. Microstructural characterization of concrete prepared with recycled aggregates. Microsc Microanal. 2013;19(5):1222–30. https://doi.org/10.1017/S1431927613001463.
61. Aghaee K, Khayat KH. Effect of shrinkage-mitigating materials on performance of fiber-reinforced concrete – an overview. Constr Build Mater. 2021;305: 124586. https://doi.org/10.1016/j.conbuildmat.2021.124586.
62. Mao Y, Liu J, Shi C. Autogenous shrinkage and drying shrinkage of recycled aggregate concrete: a review. J Clean Prod. 2021;295: 126435. https://doi.org/10.1016/j.jclepro.2021.126435.



## Authors and Affiliations

**Vanesa Ortega-López[1,2] · Flora Faleschini[2] · Juan M. Manso[1] · Víctor Revilla-Cuesta[1,2]**

✉ Víctor Revilla-Cuesta
vrevilla@ubu.es

1 Department of Civil Engineering, Escuela Politécnica Superior, University of Burgos, C/Villadiego S/N, 09001 Burgos, Spain

2 Department of Civil, Environmental and Architectural Engineering, University of Padova, Via Francesco Marzolo 9, 35131 Padua, Italy